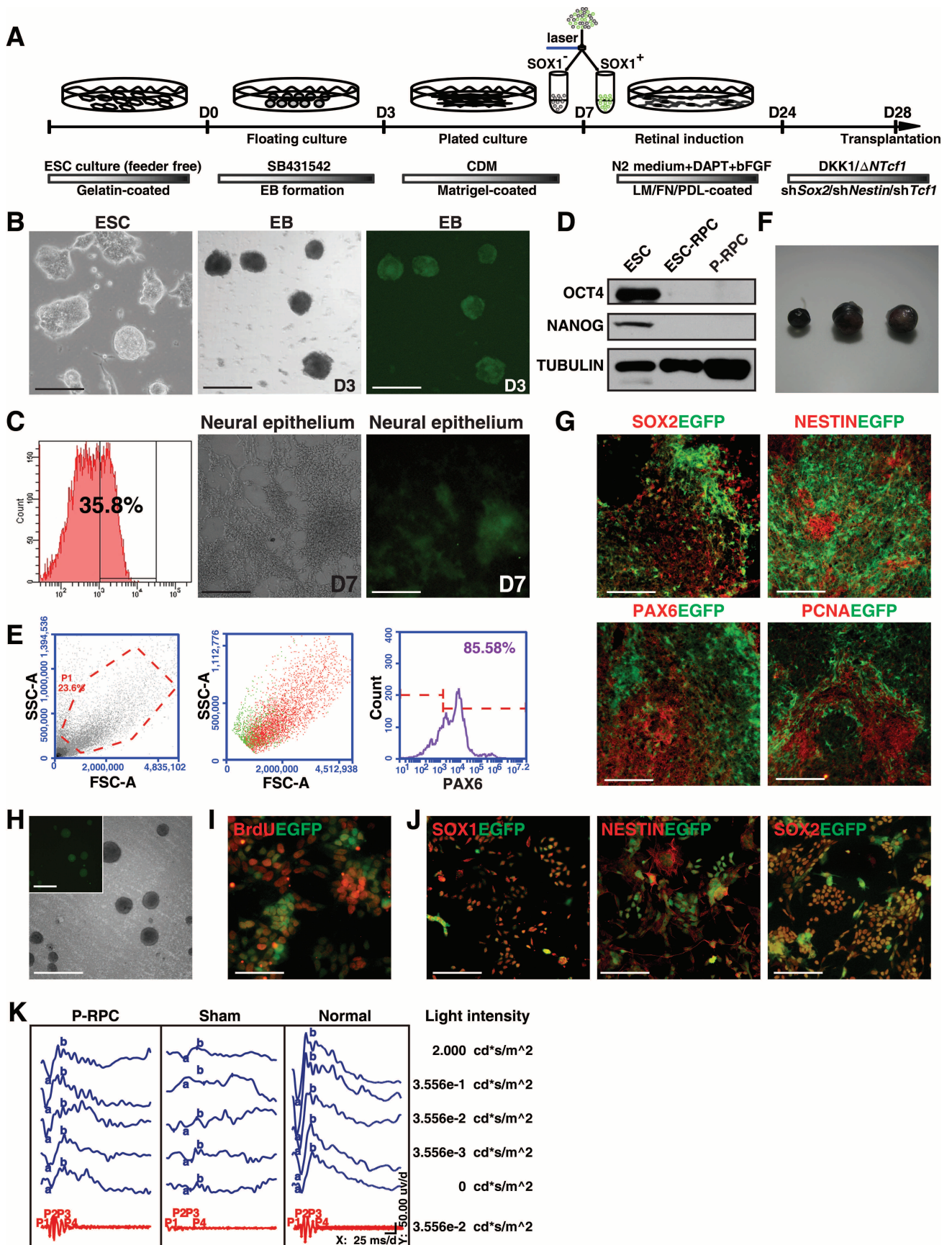


Supplemental information

**Tcf7/ β -catenin-Sox2-Nestin cascade determines tumorigenicity and
function of ESC-derived retinal progenitors**

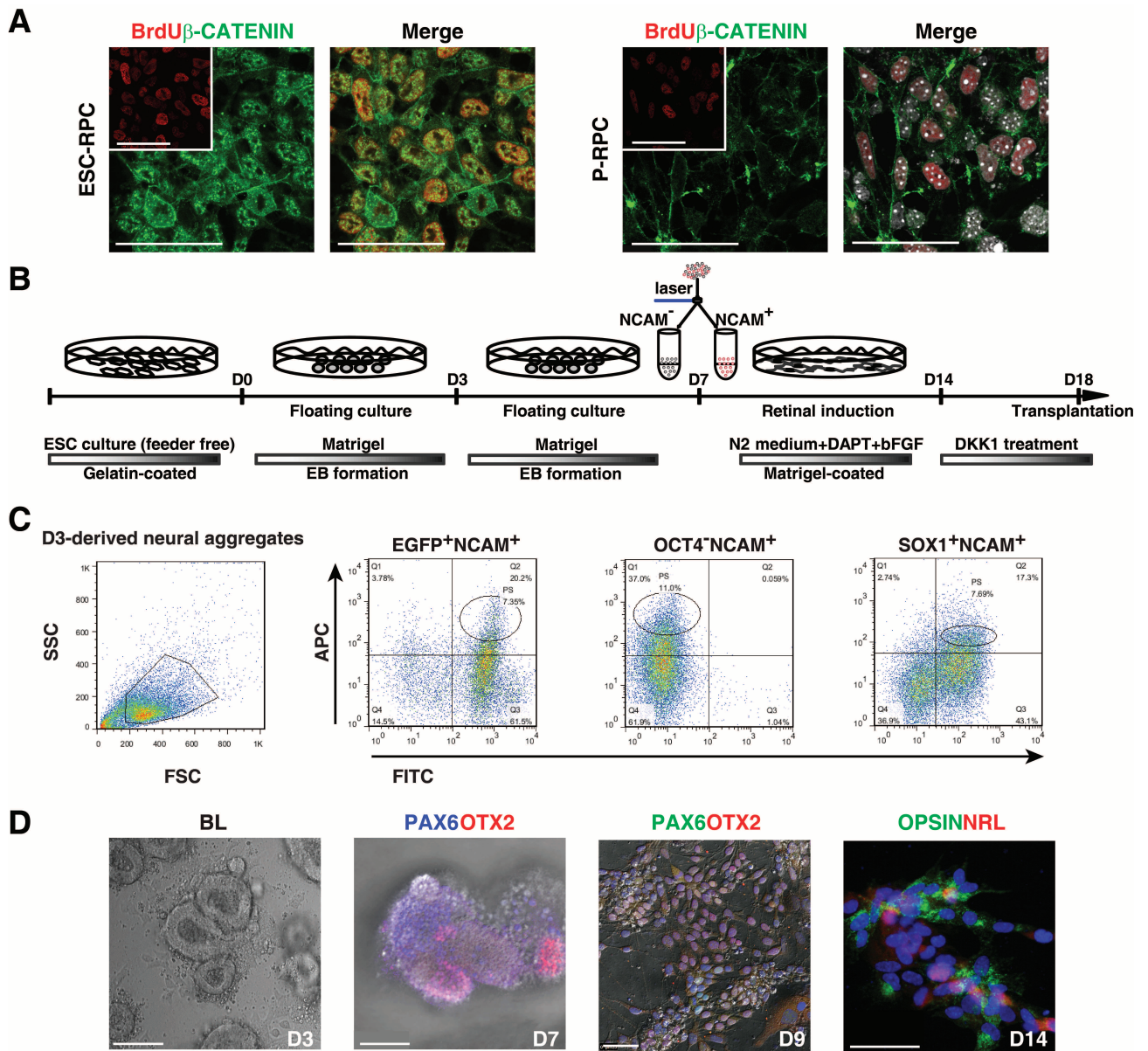
Lu Cui, Yuan Guan, Zepeng Qu, Jingfa Zhang, Bing Liao, Bo Ma, Jiang Qian,

Dangsheng Li, Weiye Li, Guo-Tong Xu & Ying Jin



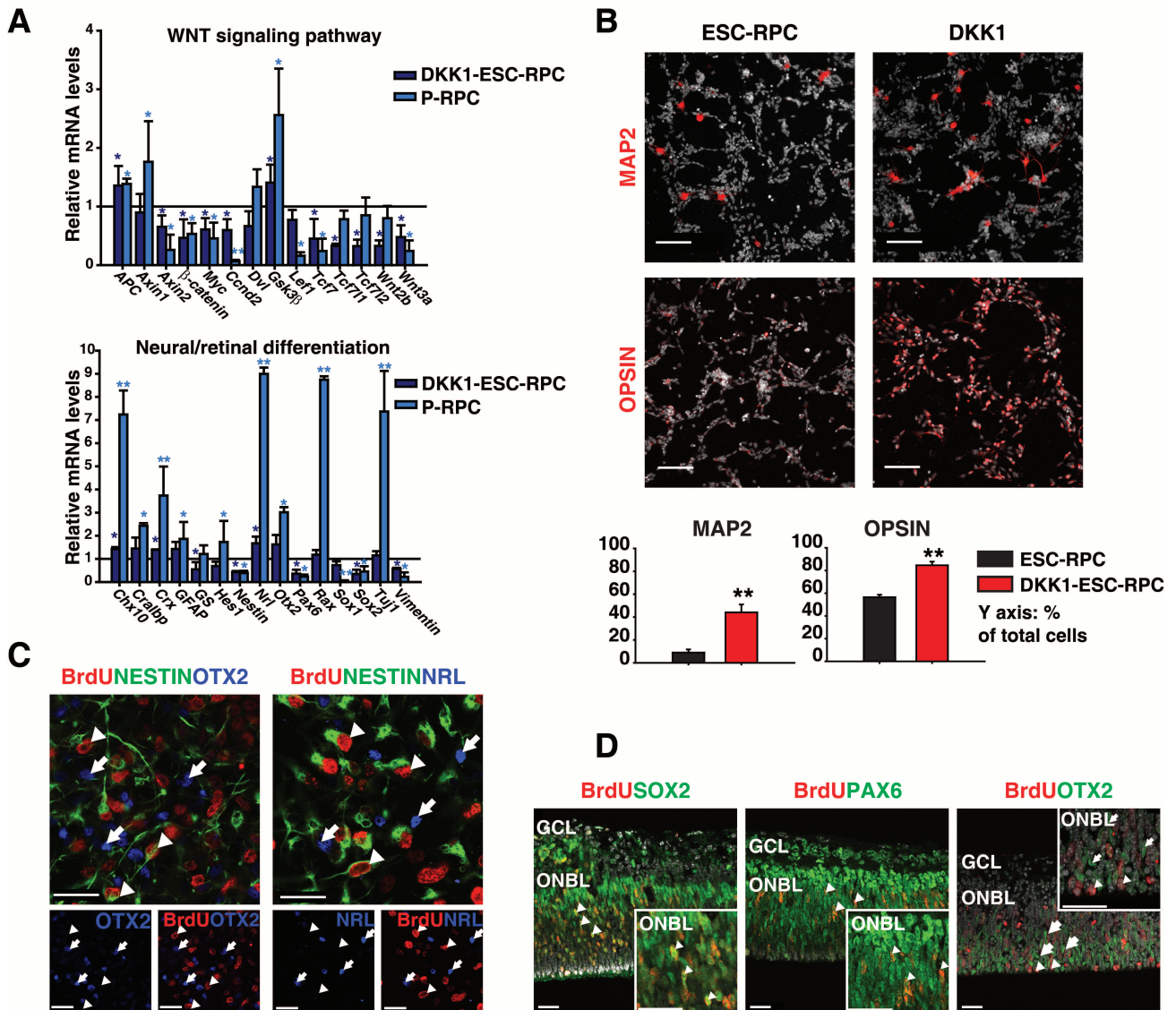
Supplemental Figure 1

Differentiation of ESCs into RPCs via a FACS selection process and further lineage-restricted induction. (A) The schematic diagram of the multi-step differentiation of mouse ESCs (46C) into RPCs. (B) The bright field image of mouse ESCs and embryonic bodies (EBs) 3 days after differentiation (D3). The fluorescence image of EGFP⁺ neural subsets in EBs is also shown. (C) Purification of the SOX1.EGFP⁺ neural epithelium by FACS from ESC derivatives at day 7 (D7) of neural differentiation in the SFEB/CDM. (D) Western blots determining endogenous expression of OCT4 and NANOG protein levels. TUBULIN serves as a loading control. (E) Representative gating strategy of FCM analysis and histogram showing 85.58% PAX6⁺ cells (red). (F) Comparison of the size of eyeballs between a normal eye (left) and ESC-RPC engrafted eyes (two at the right). (G) Immunofluorescence staining for sections of eye tumors. (H) EGFP⁺ cells were isolated from the ESC-RPCs^{EGFP} derived tumors by FACS and neurosphere formation assays were conducted by the suspension culture. (I) The BrdU incorporation assay for isolated EGFP⁺ tumor cells. (J) Immunofluorescence staining of isolated EGFP⁺ cells from eye tumors for SOX1, NESTIN and SOX2 (red), respectively. (K) Representative scotopic ERG responses (blue lines) and OPs responses (red lines) in transplanted and control eyes. The stimulus flash intensities used to activate photoreceptors are indicated along the right side. The calibration on the right indicates 50 μ V/d vertically and 25 ms/d horizontally. Scale bars, 100 μ m (B-C, G-H, J); 50 μ m (I).



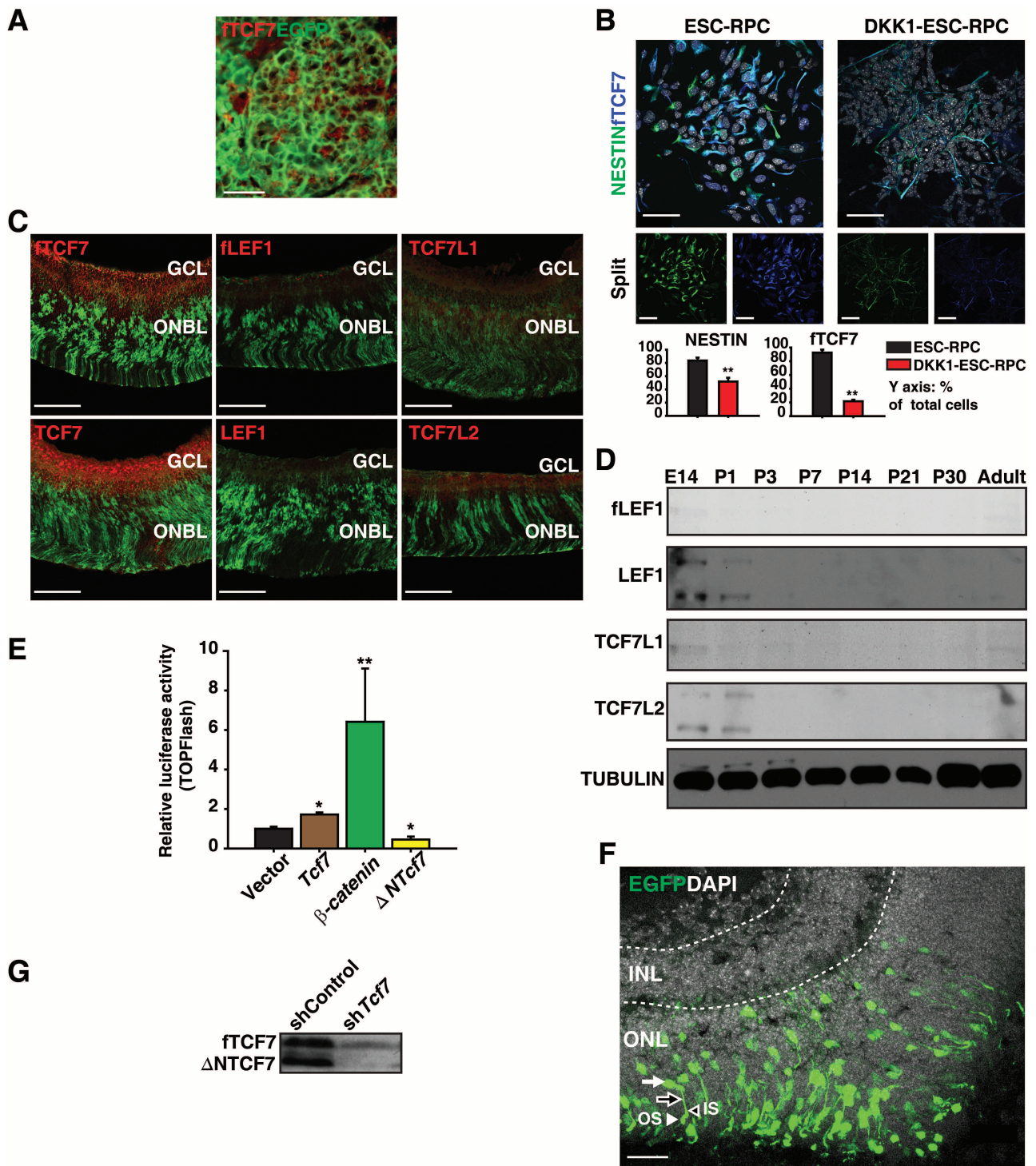
Supplemental Figure 2

The activation of canonical WNT signaling exists in the different ESC line derived RPCs. (A) The confocal image of immunofluorescence staining for β -CATENIN proteins and incorporated BrdU in ESC-RPCs and P-RPCs. DAPI is set as a grey color. Scale bars, 50 μ m. (B) The Schematic diagram of the SFEB/Matrigel method for the differentiation of additional lines of ESCs into RPCs. (C) Representative enrichment strategy of FCM plot in D3^{EGFP}, ESC^{Oct4.EGFP} and ESC^{Sox1.EGFP} derived aggregates. (D) The bright field image and immunostaining of the ESC^{Oct4.EGFP} derived cells at different differentiation stages. Scale bars, 50 μ m.



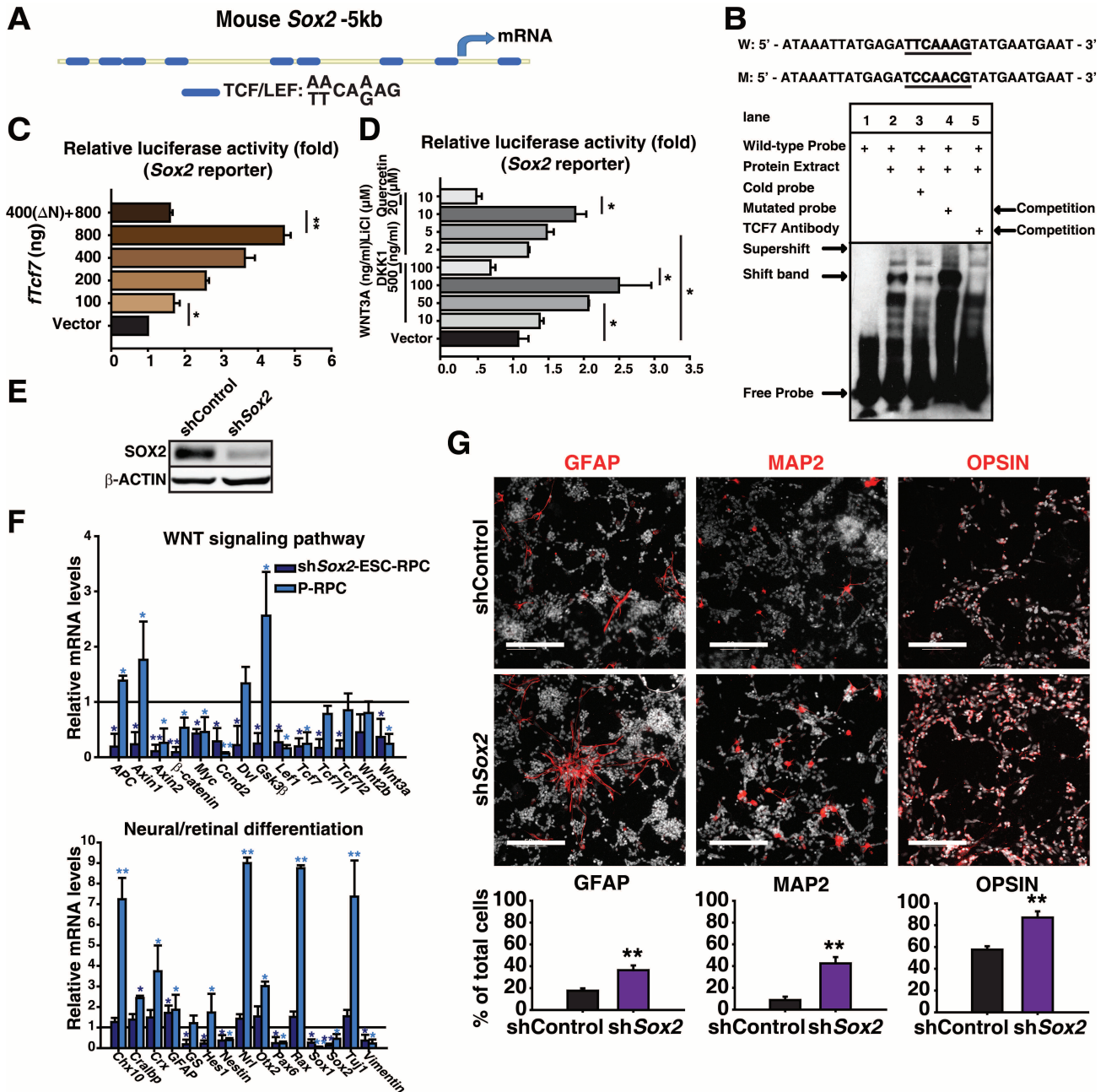
Supplemental Figure 3

Inhibition of canonical WNT signaling promotes differentiation of ESC-RPCs into more mature retinal cells. (A) Relative gene expression levels in P-RPCs and DKK1 treated ESC-RPCs were determined by qRT-PCR and compared to those in untreated ESC-RPCs, which were set at 1.0. Mean \pm SD; analysis of variance (ANOVA); * $P < 0.05$. (B) DKK1 treatment up-regulates the percentage of cells expressing MAP2 or OPSIN. DAPI is set as a grey color. Scale bars, 50 μ m. Bar charts are the quantitative analysis of the corresponding staining. Mean \pm SD; t test; ** $P < 0.01$. (C) Representative images of coimmunostaining of BrdU and NESTIN with OTX2 or BrdU and NESTIN with NRL in DKK1-ESC-RPCs. Arrowheads indicate BrdU⁺/NESTIN⁺ cells; arrows indicate post-mitotic OTX2⁺ or NRL⁺ cells. Scale bars, 25 μ m. (D) Representative images of immunostaining of BrdU with SOX2 or PAX6 or OTX2 in the neonatal mice retina. Arrowheads indicate proliferating cells; arrows indicate post-mitotic cells. Scale bars, 25 μ m. ONBL: outer neuroblastic layer.



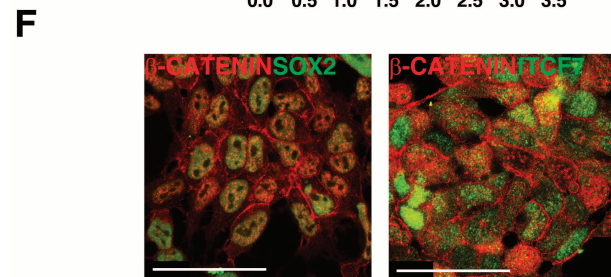
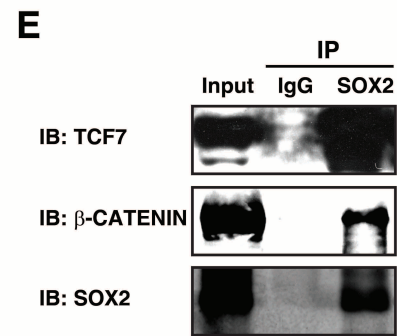
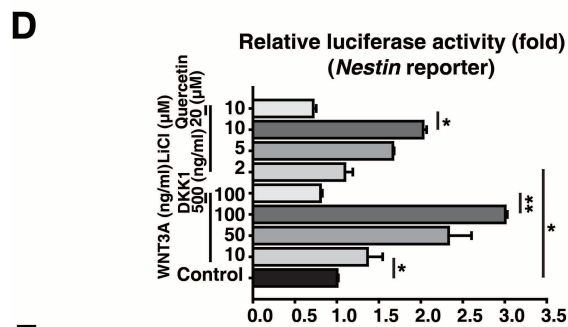
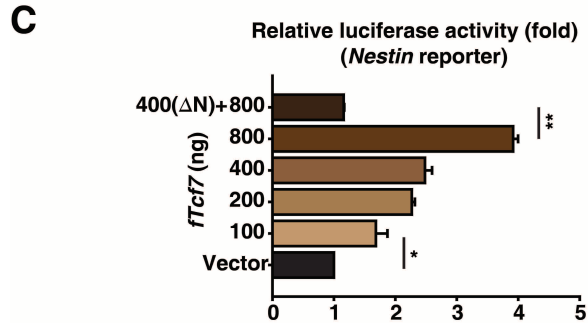
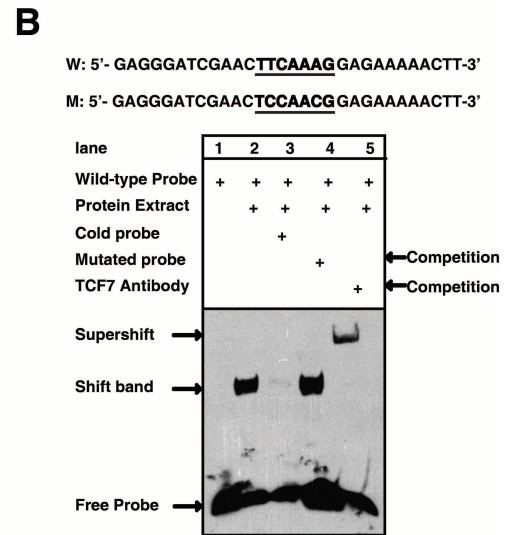
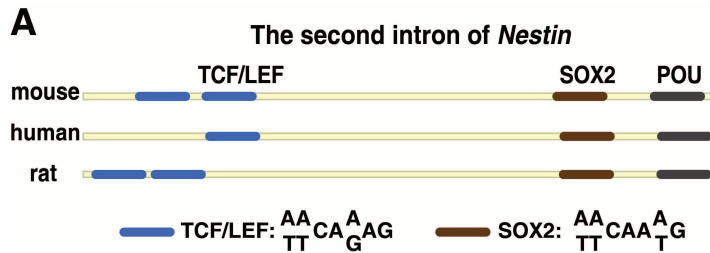
Supplemental Figure 4

TCF7 plays a key role in early retinal development and ESC-RPCs. (A) The expression of fTCF7 in ESC-RPC^{EGFP} derived tumors was analyzed by immunofluorescence staining. (B) Immunofluorescence staining shows the effect of DKK1 on the percentages of NESTIN⁺ or fTCF7⁺ ESC-RPCs. DAPI is set as grey color. Bar charts are the quantitative analysis of the corresponding staining. (C) Representative images of immunofluorescence staining for the expression pattern of TCF/LEF factors in the retina of a *Nestin.EGFP* transgenic mouse at P1. (D) Representative western blot for the expression of TCF/LEF factors except TCF7 proteins in mouse retina from E14d to the adult. (E) TOPFlash assays were performed to measure the activity of TCF7 in HEK293 cells, stimulated with the WNT3A-containing medium for 6 hours. (F) A typical image for injected Δ NTcf7-ESC-RPCs to integrate into the recipient retina three weeks after transplantation is illustrated. An integrated donor cell having the rod cell morphology is indicated (the filled arrow for the nucleus; the open arrow for the outer process; the open arrowhead for the IS; the filled arrowhead for the OS). ONBL: outer neuroblastic layer. (G) The validation of the silencing of *Tcf7* expression in ESC-RPCs was made by the western blot analysis. Data are shown as Mean \pm SD; *t* test (B); ANOVA (E); * *P* < 0.05; ** *P* < 0.01. Scale bars, 50 μ m (A, B), 100 μ m (C), 25 μ m (F).



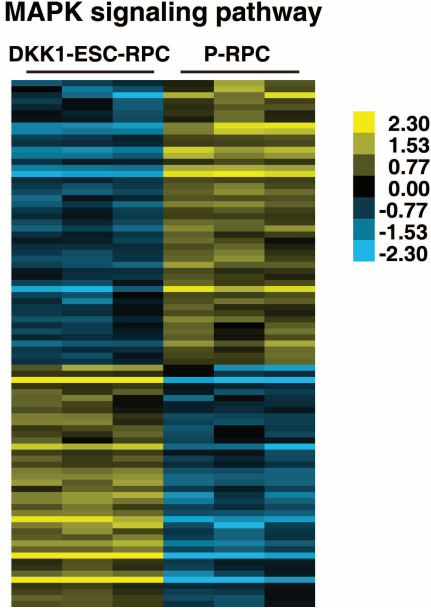
Supplemental Figure 5

The expression of *Sox2* are directly regulated by TCF7 and involved in determining the fate of ESC-RPCs. (A) The schematic representation of the binding sites of TCF/LEF transcription factors on the -5 kb promoter of the mouse *Sox2* genes (N-2 enhancer). (B) EMSA was carried out using the biotin-labeled wild-type as well as the mutated (underlined nucleotides) *Sox2* promoter probe. (C) TCF7 dose-dependently activated the *Sox2* promoter. (D) Luciferase assays with the *Sox2* promoter using WNT activators (WNT3A and LiC) as well as the WNT inhibitors (DKK1 and Quercetin). (E) Validation of the effect of *Sox2* RNAi in ESC-RPCs by western blot analysis. (F) Effects of sh*Sox2* on the gene expression in ESC-RPCs. Values in cells infected with the shControl are set at 1.0. (G) Immunofluorescence staining analysis of GFAP, MAP2 and OPSIN in sh*Sox2*- and shControl ESC-RPCs. DAPI is set as a grey color. Data are shown as mean \pm SD; ANOVA (C, D, F), *t* test (G); * $P < 0.05$, ** $P < 0.01$. Scale bars: 100 μ m (G).



Supplemental Figure 6

The expression of *Nestin* is directly controlled by WNT/TCF7 signaling and TCF7, SOX2 and β-CATENIN form protein complexes in ESC-RPCs. (A) The schematic representation of an evolutionally conserved sequence in the *Nestin* gene promoters (2nd intron) containing SOX2 (brown boxes) and TCF/LEF binding sites (blue boxes). (B) EMSA was conducted using either the biotin-labeled wild-type *Nestin* probe or a mutated probe (underlined nucleotides). (C) TCF7 dose-dependently activated the *Nestin* promoter. (D) The *Nestin* promoter activity was activated by WNT activators (WNT3A and LiCl) and blocked by WNT inhibitors (DKK1 and Quercetin) as determined by luciferase assays conducted in HEK293 cells. (E) The representative result of coimmunoprecipitation assays among TCF7, SOX2 and β-CATENIN proteins conducted in HEK293 cells. (F) Colocalization of TCF7, SOX2 and β-CATENIN proteins is illustrated by confocal images of immunostaining. Data are shown as mean ± SD; ANOVA (C, D); * $P < 0.05$, ** $P < 0.01$. Scale bars: 50 μm (F).



Supplemental Figure 7

The comparison of MAPK signaling gene expression patterns between DKK1 ESC-RPCs and P-RPCs ($P < 0.05$; Fold Change > 2).

Supplemental methods

ESC culture and differentiation into retinal progenitor cells (RPCs).

Sox1.EGFP knock-in (46C) mouse ESCs from Austin Smith were cultured on mitomycin C (Sigma-Aldrich) treated mouse embryonic fibroblasts as described previously (1) and were used for the RPC induction experiments. ESCs were suspended in the serum free differentiation medium (2-4) for 3 days to form embryoid bodies (EBs) in the presence of SB431542, an inhibitor of activin receptor-like kinase family (ALK4, 5 and 7), to block Nodal signaling. Then, EBs were plated on Matrigel-coated culture dishes in the chemical defined medium (CDM). At day 7 of the differentiation, Sox1⁺ neural progenitor cells (NPCs) (35.8%) were purified by fluorescence-activated cell sorting (FACS). The sorted cells were cultured in the N2 medium supplemented with 10 μ M DAPT (Calbiochem) and 20 ng/ml bFGF for further induction of retinal progenitor lineages until day 24.

In addition, three additional different mouse ESCs lines, namely D3 ESC line expressing EGFP constitutively (D3^{EGFP}), ESCs carrying an *Oct4.EGFP* transgene (ESC^{Oct4.EGFP}) (5), and an ESC line (kindly provided by Austin Smith) expressing EGFP under the control of the endogenous Sox1 locus and generated under 2i condition (2i-ESC^{Sox1.EGFP}) (inhibitors of Fgf/Ras/Mek

signaling and GSK3), were used to generate ESC-RPCs through the SFEB/Matrigel method (6). ESCs were suspended in the serum free differentiation medium supplemented with 2% (v:v) Matrigel at D0. The medium was changed at D3. On day 7, the cell aggregates were digested in the papain system, sorted by FACS. Then the enriched neural lineage cells were replated in the N2 medium supplemented with 10 μ M DAPT and 20 ng/ml bFGF, cultured until day 14. The FACS enrichment strategy differed for the derivatives of the 3 ESC lines: EGFP⁺ and PSA-NCAM⁺ cells were collected for D3^{EGFP} cell line; Oct4⁻ and PSA-NCAM⁺ were sorted for ESC^{Oct4.EGFP} cell line; Sox1⁺ and PSA-NCAM⁺ cells were selected for 2i-ESC^{Sox1.EGFP} cell line.

DKK1 treatment (100 ng/ml), overexpression of $\Delta NTcf7$ and silencing total *Tcf7*, *Sox2* or *Nestin* in ESC-RPCs were performed 4 days before in vitro assay or subretinal transplantation.

Dissociation of the retinal tissue. Retinal cells from P1 C57BL/6 mice with a constitutively expressed *EGFP* transgene were digested in the papain dissociation system (Roche). Then cells were suspended in GMEM supplemented with DNase (0.005%) and kept on ice prior to subretinal

transplantation, FCM analysis and collect in TRIzol for microarray analyses.

Flow cytometric analysis. For 46C ESCs, retina committed aggregates were cultured in the CDM until day 7. For retinal tumor tissues, they were separated and washed with HBSS carefully. Then the aggregates and tumor tissues were washed for 3 times, dissociated in the papain dissociation system (Roche), triturated mechanically with fire-narrowed Pasteur pipettes. After neutralization, the cells were resuspended in HBSS containing 0.1% of BSA, and filtrated through a cell strainer (BD Biosciences). To separate two distinct cell populations (EGFP⁺ and EGFP⁻), cells were sorted using a FACS Aria cell sorter and FACS Diva software (BD Biosciences). Gates for each population were set so that two subsets sorted based on EGFP expression would not overlap when reanalyzed.

For flow cytometric analysis, cultured cells and neural retinae were dissociated by TrypLE (Life Technologies) and the papain dissociation system, respectively, into single cell suspension, then fixed by 4% paraformaldehyde and permeabilized by ice-cold Methanol. Before staining, the sample cells were washed in PBS containing 1% BSA and 0.03% NaN₃ (wash buffer) and then stained by the specific antibody. After the primary antibody was added, the cells were incubated on ice for 20 min, and washed twice with wash

buffer. Then the second antibody was added, the cells were incubated on ice for 20 min, and washed twice with wash buffer. Before analysis, samples were filtered through cell strainer caps (35 μm mesh; BD Biosciences) and then performed on the BD Accuri C6 flow cytometer and the C6 software program (BD Biosciences).

BrdU incorporation analysis. To examine the proliferation capacity of differentiated cells, ESC-RPCs were plated onto coverslips coated with poly-D-Lysine (Millipore), laminin (BD Biosciences) and fibronectin (BD Biosciences). 5-bromo-2'-deoxyuridine (BrdU, Sigma-Aldrich) was added at the final concentration of 10 μM . Four hours later, cells were fixed for further immunostaining assay.

Immunofluorescence staining and quantification. Immunostaining analyses were carried out for the detection of cell-specific markers and/or BrdU. Cells were seeded onto glass coverslips and fixed with 4% paraformaldehyde.

Mice were anesthetized and perfused intracardially with 0.1 M phosphate buffer saline (PBS) followed by 4% paraformaldehyde in PBS at 4 $^{\circ}\text{C}$. Retinae were removed and embedded in optimum cutting temperature compound on

liquid nitrogen. Cryosections (10-20 μm) were cut on a cryostat (Leica). Then slides and sections were stained as described previously (7).

Primary antibodies used were as followings: Sox2 (Rabbit); Pax6 (Rabbit, Covance); Nestin (Mouse, Chemicon); Nrl (Rabbit, Chemicon); Vimentin (Rabbit, Biovision); BrdU (Rat, AbD Serotec); PCNA (Mouse, Sigma); Hes1 (Rabbit, Chemicon); Rax (Rabbit, Millipore); Otx2 (Rabbit, Chemicon); Sox1 (Rabbit, Abcam); Opsin (Mouse, Sigma-Aldrich); fTcf7 (Rabbit, Cell Signaling); Tcf7 (Rabbit, Cell Signaling). For secondary antibody staining, we used the corresponding Cy3 and FITC fluorescent-tagged antibodies (Jackson).

The population of BrdU⁺, PCNA⁺, Sox2⁺, Nestin⁺ and fTcf7⁺ cells among total differentiated cells (DAPI-labeled) was counted with an Image-Pro Plus software (Media Cybernetics). At least five fields of each coverslip were chosen randomly and three coverslips in each group were counted. Data were replicated at least three times and were expressed as mean \pm SD.

Lentivirus preparation. The full length of *Tcf7* was cloned from total cDNA of the mouse kidney by standard molecular procedures, and subcloned into lentiviral vector pRRL by primers as followings: 5'-ATG CCG CAG CTG GAC TCG-3' and reverse: 5'-CTA GAG CAC TGT CAT CGG-3'. The $\Delta NTcf7$

overexpression vector was generated using the pCDF1-MCS2 expression vector. The cDNA sequence encoding the $\Delta NTcf7$ isoform, which lacks the amino-terminal β -catenin binding domain, was amplified by PCR using cDNAs of mouse ESCs as a template. Primers used for PCR are as followings: $\Delta NTcf7$ forward: 5'-ATG TAC AAA GAG ACT GTC TAC T-3' and reverse: 5'-GAG CAC TGT CAT CGG AAG GAA C-3'.

Lentiviruses were collected and concentrated by spinning in a centrifuge at 1000 g for 5 min (keep viruses cold). Then supernatant was filtered through a 0.45 μ m filter. Different batches of viruses were collected and spun in refrigerated ultracentrifuge (Hitachi, CP80MX) at 100,000 g for 2 hours. Pellets were resuspended in PBS containing BSA, followed by titer, aliquot and store at -80 °C.

Lentivirus-mediated shRNA interference. Gene-specific regions of 21 bases for RNA interference were designed based on the RNAi Consortium protocol. Oligonucleotides were cloned into the pLKO.1 clone vector (10878, Addgene). All sequences were analyzed by BLAST search to minimize the off-target effect. The plasmid pLKO.1 - TRC was used as a control (10879, Addgene). The sequences used were as followings: sh*Tcf7*: 5' - TTC TCC ACT CTA CGA ACA TTT -3'; sh*Sox2*: 5' - AAG CTG AGA ATT TGC CAA TAT -

3'; sh*Nestin*: 5' - AGA AGA CCA GCA GGC GTT TAG -3'. Twenty-four hours after lentiviral particle infection, puromycin was used to select for cells that stably expressed the shRNA of interest. The efficiency of RNAi was validated by qPCR or western blot analysis at ≥ 4 days post infection.

RNA sample preparation, RT-PCR and qRT-PCR analyses. Total RNA was extracted from cultures using TRIzol (Invitrogen) followed by chloroform extraction according to the manufacturer's protocol. For RT-PCR analysis, two μg of total RNA was reverse-transcribed using RevertAidTM M-MuLV RT kit (Fermentas) and Oligo d(T)₁₈ primers according to manufacturer's instructions. PCR performed on 1/20 of the final cDNA volume using the 2xTaq PCR master mix (Tiangen). Reactions were performed at 60 °C for 30 cycles.

Real-time qRT-PCR was performed with SYBR[®] Green qPCR Premix Ex TaqTM II with ROX (TaKaRa) according to manufacturer's instructions. Signals were detected on an ABI PRISM 7900 machine (Applied Biosystems). QRT-PCR was performed for various genes and results were normalized to *Gapdh* levels.

Sequences of primers used in this study are provided in Supplemental Table

5.

Protein sample preparation and western blot analysis. Samples were collected and lysed in ice-cold a radioimmune precipitation assay buffer (RIPA) supplemented with protease inhibitor phenylmethanesulfonyl fluoride (PMSF, Shenergy Bicolor Bioscience Technology Company) and cocktail (Sigma-Aldrich). After 30 min incubation on ice, extracts were clarified by centrifugation at 12000 g for 20 min at 4 °C and stored at -80 °C. Protein concentrations were determined by a protein assay kit (Bio-Rad). Western blot analysis was carried out as previously described (7). Specific signals were detected using fluorescence-conjugated secondary antibodies (LI-COR), and scanned by the Odyssey 9120 Infrared Imaging System (LI-COR).

Luciferase assays. Cells were seeded at a density of 1.2×10^5 per well into 24-well plates 24 hours before transfection. To determine the endogenous activity, cells were transfected with reporter plasmids (250 ng) and vector pRL-TK (10 ng, Promega) as a control for the transfection efficiency using Lipofectamine 2000 (Invitrogen). Eighteen hours after transfection, cells were stimulated with the Wnt3a-containing medium for 6 hours. Then, cells were lysed and luciferase activities were evaluated with the Dual-Luciferase Assay

System (Promega) according to the manufacturer's recommendations.

Chromatin immunoprecipitation (ChIP) assays. The ChIP analysis was performed as described previously (7) with the anti-Tcf7 antibody. Immunoprecipitated DNA fragments were analyzed by PCR amplification using primers for *Sox2* and *Nestin* genes. Ten percent of the total genomic DNA from the nuclear extract was used as the input. The primers used are as followings: *Sox2* forward: GCA CGA CCG AAA CCC TTC TT, reverse: GCT GCC ATC TCC CTG TCC AA; *Nestin* forward: GAC ATT GAG GCT GAA GGA GC, reverse: TCG GTT TGT TTG GGG CAC TT; *DHFR* forward: CTG ATG TCC AGG AGG AGA AAG G, reverse: AGC CCG ACA ATG TCA AGG ACT G.

Electrophoretic mobility shift assays (EMSAs). Nuclear extracts isolated from HEK293 overexpressing *Tcf7* for 2 days were prepared and EMSAs were performed as described previously (8). In brief, oligonucleotide probes were synthesized and labeled with biotin at the 3' end of the forward oligonucleotide. For the competitive assay, an additional 200-fold molar excess of the unlabeled probe was added. For the super-shift analysis, Tcf7 antibody (2 μ l per reaction) was added.

Supplemental references

1. Ying QL, Stavridis M, Griffiths D, Li M, and Smith A. Conversion of embryonic stem cells into neuroectodermal precursors in adherent monoculture. *Nat Biotechnol.* 2003;21(2):183-6.
2. Ikeda H, Osakada F, Watanabe K, Mizuseki K, Haraguchi T, Miyoshi H, Kamiya D, Honda Y, Sasai N, Yoshimura N, et al. Generation of Rx+/Pax6+ neural retinal precursors from embryonic stem cells. *Proc Natl Acad Sci U S A.* 2005;102(32):11331-6.
3. Hirami Y, Osakada F, Takahashi K, Okita K, Yamanaka S, Ikeda H, Yoshimura N, and Takahashi M. Generation of retinal cells from mouse and human induced pluripotent stem cells. *Neuroscience letters.* 2009;458(3):126-31.
4. Kuwabara T, Hsieh J, Muotri A, Yeo G, Warashina M, Lie DC, Moore L, Nakashima K, Asashima M, and Gage FH. Wnt-mediated activation of NeuroD1 and retro-elements during adult neurogenesis. *Nature Neuroscience.* 2009;12(9):1097-U6.
5. Yang H, Shi L, Wang BA, Liang D, Zhong C, Liu W, Nie Y, Liu J, Zhao J, Gao X, et al. Generation of genetically modified mice by oocyte injection of androgenetic haploid embryonic stem cells. *Cell.* 2012;149(3):605-17.
6. Eiraku M, Takata N, Ishibashi H, Kawada M, Sakakura E, Okuda S, Sekiguchi K, Adachi T, and Sasai Y. Self-organizing optic-cup morphogenesis in three-dimensional culture. *Nature.* 2011;472(7341):51-6.
7. Li L, Sun L, Gao F, Jiang J, Yang Y, Li C, Gu J, Wei Z, Yang A, Lu R, et al. Stk40 links the pluripotency factor Oct4 to the Erk/MAPK pathway and controls extraembryonic endoderm differentiation. *Proc Natl Acad Sci U S A.* 2010;107(4):1402-7.
8. Li X, Zhu L, Yang A, Lin J, Tang F, Jin S, Wei Z, Li J, and Jin Y. Calcineurin-NFAT signaling critically regulates early lineage specification in mouse embryonic stem cells and embryos. *Cell stem cell.* 2011;8(1):46-58.

Supplemental Table 1

mouse RT-PCR primer

Pax6 ACCTCCTCACTCGTGCC
CCTGAATACCCAAGTCTGCT
Rax CGGCATCCTAGACACCTTTCC
ACTTAGCCCGTCCGTTCTG
Hes1 TCTACACCAGCAACAGTGG
TCAAACATCTTTGGCATCAC
Isl1 GTGCGGACTGTGCTCAAC
AGCCTGGTCTCCTTCTG
Calb TGCCAGCAACTGAAATCC
CTTCCCTCCATCCGACAA
Chx10 TGGTCCACGGTGTAACT
GAGGGCTCACCAGCAGTA
Otx2 CCAAATCTACCCACCAAG
TTCTGACCTCCATTCTGC
Crx GGGCACAAGTATGAAGT
GCTGGTAGTCTTGGGTTCT
Nrl ATGGCTCAGTGCCTTG
TGGTTGGGTTGGGTAG
Gapdh GGCAAGTTCACGGCACA
CGCCAGTAGACTCCACGACA

mouse QRT-PCR primer

APC GCCAGGACATGGAGAAGCGTGC
CCACACGTGTAGCTGGACTCTGAC
Ctnnb1 AGATGTGGACACTCCCAAG
GCTGGTGAACCATAACAGCA
Gsk3b CCACAGAACTCTTGTGGA
CCAACTGATCCACACCCTG
Myc CCCATTGCAGCGGGCAGACA
CATCGTCGTGGCTGTCGGGG
Wnt2b GTCGCACGGCTGTTCCGAGATT
GACGCGCCTGCGGTACCTA
Wnt3a TGAAGCAGGCTCTGGGCAGC
GCTGACTCCCGGGTGGCTTT
Sox2 CCTTCTCCAGTTCGAGTCC
CCCCGTGGTTACCTCTTCC
Nestin CCCTCCATGTCGCTGGTCT
GTCAGTTCGCCGCTACTCC
Vim GCCGAGGACATCATCGCGCT
GCTCCTGGATCTTTCATCGTGC
Pax6 GGCTTACTCCCTCCGATTGC
CAGCTTGGTGGTGTCTTTGTCA
Sox1 AAGATGCACAACCTCGGAGATCAG
TGTAATCCGGGTGTTCTTCAT
Otx2 AGACAGTGGGGAGATGGACG
CAGCAGAATGGAGGTGAGAACA
Rax AGTTGCTGCGAGCCCTGTG
AGGTGAATTTCCGTTTGG
Hes1 GCGTGTGGGAAATACCG
GGTCATGGCGTTGATCTGG
Crx CCAGCGGAATCACTCTTT
GCTGAGGGTAGGAAACAC
Chx10 GACGGCCAGTCCGATTCCG
CCCAGGCGTAGACATCTGGGT
Nrl CCACTACCACAACCGAAACCC
GCTTCTGCTCTGCCAACG
Cralbp AGAGGGGGTGGGCACATTCCG
TCCCTCACCGCCTCATCCCG
GS ATCGTGGAGGCTCACTACCG
CCCAAAGTCTTGCATACCC
Tuj1 GCTCGTCCACTCTTATAGA
CGGCTTCGCCCACTTAC
GFAP CAGCTTACGGCCAACAGT
TCCAGCGATTCAACCTTT
Gapdh GGCAAGTTCACGGCACA
CGCCAGTAGACTCCACGACA
Dvl TGCAGTAACCTCGCATCCCTGAA
GATGGCTGCTCCGTGTGGACC
Axin1 GAGGGAGCCCGTCAACCCCT
TGGCATTGGTAAGTGCGAGGA
Axin2 AGCGCCAACGACAGCGAGTT
CAGGGCGTGGTCTCGGAAA
Lef1 TTCAGGCAACCCATCCCA
TCTTCCGTGCTAGTTCATAG
Tcf7 AGGCGAGGAACAGGACGATA
TTCTCCATGTAAGTGGACGC
Tcf7l1 GCTGGGCTTGGAGGCAAGGG
GGCGGAACCTCCGGACCTT
Tcf7l2 ACCCGGCAAACCTGAACTGT
ACAGGAGGCGAAACATCGCACT
Ccnd2 CGCTCTGTGCGCTACCGACTT
AGGGGTGGTGGCTTGGTCCG
Oct4 CATTGTTGTCGGCTTCTCTCC
GCTCACCTGGGCGTTCT
Nanog ACCTTCGGAAGAGCAGTC
GAGGCAAAAGATAAGTGGG
Rex1 TCCTCAGTCTGGGGCTAAT
GAAGAAAACGGCAAAGCAAGT

Gene Symbol	ESC-RPC/P-RPC Fold Change	Gene Symbol	ESC-RPC/P-RPC Fold Change	Gene Symbol	ESC-RPC/P-RPC Fold Change
Fzd5	0.111907528	Myc	2.513568809	Sfrp1	5.294090197
Frat2	0.141845346	Mapk8	2.565460726	Fzd9	5.714392001
Camk2d	0.277011519	Mapk10	2.592324797	Fzd1	6.037078196
Ccnd1	0.312599136	Wnt7b	2.612647383	Wnt5a	6.03936811
Trp53	0.337103401	Nfat5	2.675575978	Sox17	15.64775313
Rock1	0.361971387	Nkd1	2.76926771	Ccnd2	22.83675928
Btrc	0.439038591	Vangl2	2.80753009		
Ppp3ca	0.443690545	Sfrp2	2.865270124		
Zranb1	0.475374641	Tcf7l1	2.933009748		
Prkx	0.483443698	Daam1	2.94821772		
Senp2	0.485741315	Plcb3	2.955015455		
Ppp3cc	0.499634634	Tcf7l2	3.017497463		
Tcf7	2.217178	Axin2	3.23156096		
Tbl1xr1	2.140452271	Fzd7	3.51521587		
Daam2	2.383522378	Fzd10	5.176786312		

Supplemental Table 2

Gene expression fold change in WNT signaling pathway between ESC-RPC and P-RPC.

Donor cells	Tumor		Integration		Failure	
ESC ^{Oct4.EGFP} -RPC	11/16	68.75%	5/16	31.25%	0/16	0.00%
DKK1-ESC ^{Oct4.EGFP} -RPC	0/16	0.00%	14/16	87.50%	2/16	12.50%
2i-ESC ^{Sox1.EGFP} -RPC	9/16	56.25%	6/16	37.50%	1/16	6.25%
DKK1-2i-ESC ^{Sox1.EGFP} -RPC	1/16	6.25%	14/16	87.50%	1/16	6.25%
D3 ^{EGFP} -RPC	13/20	65.00%	7/20	35.00%	0/20	0.00%
DKK1-D3 ^{EGFP} -RPC	1/20	5.00%	18/20	90.00%	1/20	5.00%

Supplemental Table 3

Summary of transplantation results of six groups of donor cells used in this study. Failure is defined by the absence of EGFP⁺ donor cells in injected eyes.

Subretinal injection	Tumor	
<i>fTcf7</i> with recombination WNT3A protein	18/20	90.00%
<i>EGFP</i> with recombination WNT3A protein	0/10	0.00%
Sham control	0/10	0.00%

Supplemental Table 4

Summary of the tumorigenicity potential of postnatal 1 day mouse retinae 3 weeks after *fTcf7* overexpression with recombination WNT3A protein. The *EGFP* with recombination WNT3A protein and sham injection are taken as control.

Gene Symbol	DKK1-ESC-RPC/P-RPC Fold Change	Gene Symbol	DKK1-ESC-RPC/P-RPC Fold Change	Gene Symbol	DKK1-ESC-RPC/P-RPC Fold Change
Ddit3	0.230605049	Egf	0.480359297	Mras	0.484947
Fos	0.082159587	Egfr	2.885270326	Myc	2.148288303
Fasl	4.757526137	Fgf1	6.904013056	Mef2c	3.958889882
Taok1	2.011582757	Fgf14	0.382073336	Ntrk2	9.612437437
Traf6	0.385771154	Fgf17	2.702886204	Pak1	2.220838019
Atf4	0.41525902	Fgf4	79.82052108	Pla2g1b	40.92786126
Relb	0.362198363	Fgf9	0.092042213	Pla2g2c	0.326410486
Bdnf	0.212044033	Fgfr1	3.368666498	Pla2g4b	0.436448133
Cacna1d	0.24389002	Fgfr2	5.726276392	Jmjd7	0.192175489
Cacna1h	0.146651192	Fgfr3	6.381449915	Pla2g10	2.989651808
Cacna2d1	0.104835426	Gadd45a	0.413086464	Pdgfra	2.864819732
Cacna2d3	3.637411626	Gng12	2.289720993	Pdgfrb	5.129423635
Cacnb4	2.287121803	Hspb1	3.753745991	Prkx	0.474288893
Cacng2	0.407078932	Hspa1b	0.296285594	Ppm1a	0.405585856
Cacng3	0.139959319	Hspa1a	0.331589083	Ppp3ca	0.440012954
Cacng5	0.446118488	Hspa2	0.243017096	Ppp5c	0.459987761
Cdc25b	0.461837527	Ikbkb	2.09783302	Rps6ka6	2.056199616
Dusp16	0.40333118	Mapk10	2.661179621	Kras	2.656298668
Dusp6	0.158333413	Mapk11	2.453295902	Trp53	0.372890307
Evi1	7.588610402	Mapk8	2.533603547	Tgfb2	0.414374663
Tgfb3	0.413993615	Tgfb2	5.636711631		

Supplemental Table 5

Gene expression fold change in MAPK signaling pathway between DKK1-ESC-RPC and P-RPC.